Electronic Supplementary material

Ruthenium-Infused Nickel Sulphide Propelling Hydrogen Generation via Synergistic Water Dissociation and Volmer Step

*Nasrin Banu G [a], Rama Prakash M [a], Anantharaj Sengani [b], Bernaurdshaw Neppolian *[a]*

a **-** Energy & Environmental Remediation Laboratory, Department of Chemistry, Faculty of Engineering & Technology, SRM institute of Science and Technology, Kattankulathur, Chennai, Tamilnadu, India, 603 203

b **-** Department of Chemistry, Indian Institute of Technology, Kanpur, Uttar Pradesh, India, 208 016

EXPERIMENTAL

1. Materials Used

Thioacetamide and KOH were procured from SRL chemicals, Ruthenium (III) chloride hydrate was purchased from Sigma Aldrich. Ni foam of 95% - 98% porosity was procured from Vitra technologies, India. Deionized water was used wherever required. Ethanol and acetone were used for ultrasonic segregation of NiS and RuNiS for TEM and XPS. All electrochemical characterizations were carried out with Biologic SP150 electrochemical workstation inside a Faraday cage.

2. Fabrication of Ru@NiS/Ni foam

The schematic representation of fabrication of Ru@NiS/Ni foam is shown in fig. S1. A set of as-procured Ni foam pieces, each measuring 1 cm x 5 cm, were immersed in a solution comprising 40mL of water, containing 0.1M thioacetamide and 40 mM KOH. Then 100 mM of Ruthenium (III)chloride hydrate was introduced into the mixture and stirred well. Then the solution is transferred to Teflon vessels, sealed within a stainless-steel autoclave and subjected to heating at 160^{o}C for a period of 6 hours. After cooling, the resulting Ruthenium-incorporated sulfurized Ni foam pieces were washed with water and ethanol. These modified electrodes are denoted as Ru@NiS/Ni foam, and were utilized for all subsequent electrochemical characterizations. NiS/Ni foam was also prepared for comparison using the same method without adding Ruthenium precursor.

3. Preparation of Pt-C/NF

10 mg of commercial Pt-C was dispersed in 1mL solution of water-nafion-ethanol (taken in 6:3:1 volume ratio) by sonicating for 60 mins, results in uniform ink of Pt-C. About 15μL of

this homogenized ink was casted on 1 x 1 cm^2 nickel foam and dried at ambient conditions for 4 h.

4. Characterization studies

The phase and crystalline structure of NiS/Ni and Ru@NiS/Ni were meticulously characterized utilizing X-ray diffractometer (XRD) from Bruker, USA, employing Cu Kα radiation with a wavelength of 1.5418 Å. Morphological analysis of the composites was performed using Filed Emission Scanning Electron Microscopy (FE-SEM) on a Quanta 200 instrument and Transmission Electron Microscopy (TEM) on a JOEL apparatus operated at 200kV. The elemental composition of the prepared catalyst was analyzed through X-ray photoelectron spectroscopy (XPS), conducted on a k-Alpha XPS system by Thermo scientific.

5. Electrochemical HER characterizations

All HER characterizations were conducted in 1.0 M KOH solution, utilizing a Hg/HgO reference electrode and Nickel foam as counter electrode. Linear sweep voltammetry (LSV) was recorded with a sweep rate of 5 mV s^{-1} and was iR corrected (100%) by incorporating the uncompensated resistance (R_u) obtained from electrochemical impedance spectroscopic measurements (EIS). Tafel lines were derived from steady state voltammetry of potential -0.8 to -1.5 V vs. Hg/HgO. Chronoamperometry (CA) was performed at an overpotential of -1.2 V vs. Hg/HgO, to evaluate the endurance of Ru@NiS/Ni foam. All EIS measurements were carried out at -1.1 V vs. Hg/HgO, a potential at which the studied electrodes exhibited significant HER activity within the frequency range of 100 kHz to 0.1 Hz. The AC perturbation sine wave amplitude was consistently set at 10 mV for all EIS measurements. Cyclic voltammetry (CV) responses of Ni foam, NiS/Ni foam and Ru@NiS/Ni foam electrodes were obtained with increasing scan rates in the region of -1.0 to -0.85 V vs. Hg/HgO to determine double layer capacitance (C_{dl}), a key parameter indicative of electrochemically active surface area (ECSA).

Potentials were transformed to the reversible hydrogen electrode (RHE) scale where necessary. The subsequent discussion delves into the results of electrochemical and material characterizations, revealing the pivotal role of Ru incorporation for enhancing the alkaline HER performance of NiS/Ni foam.

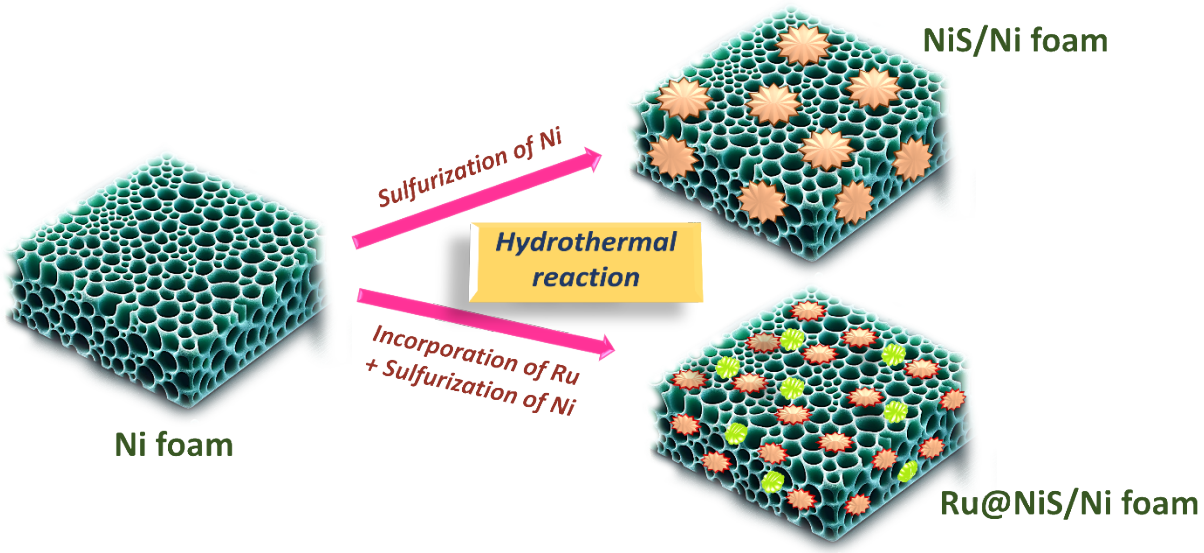

Fig. S1. Schematic representation of formation Ru incorporated NiS on Ni foam

Supporting figures and tables

6. Morphology

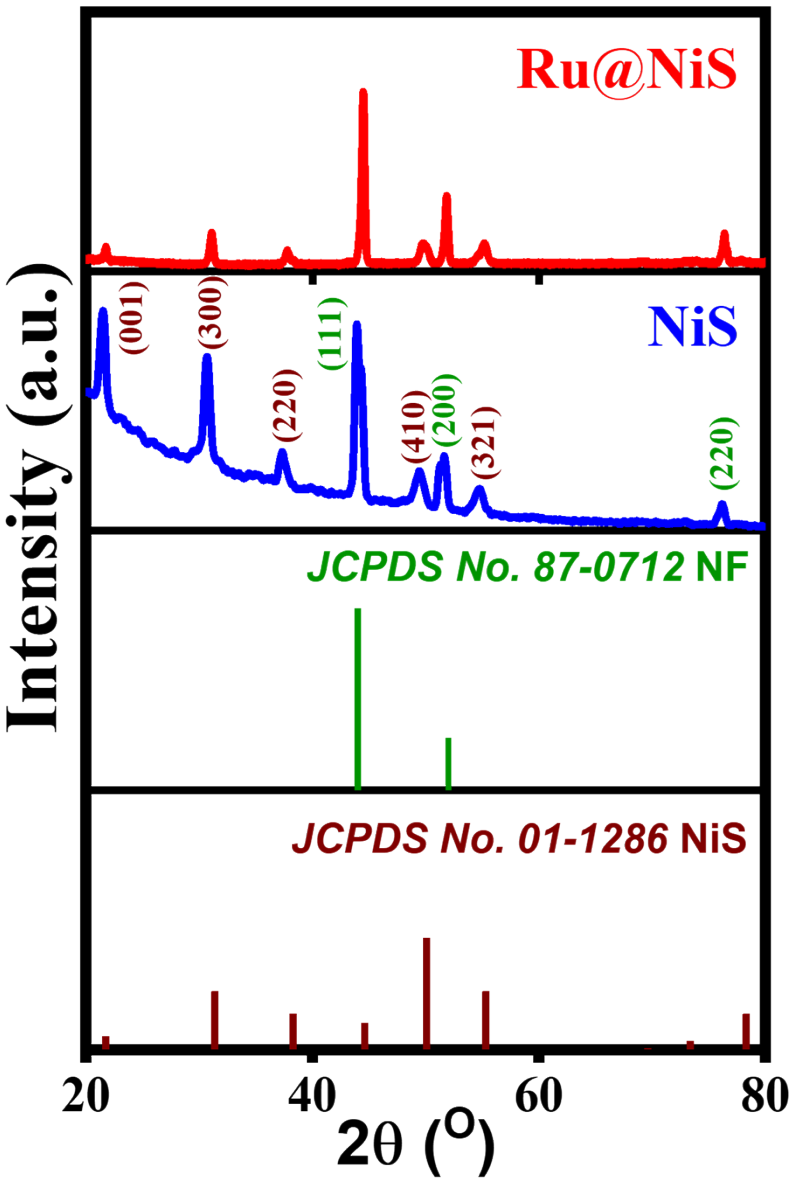

Fig. S2. XRD patterns of NiS/Ni foam and Ru@NiS/Ni foam.

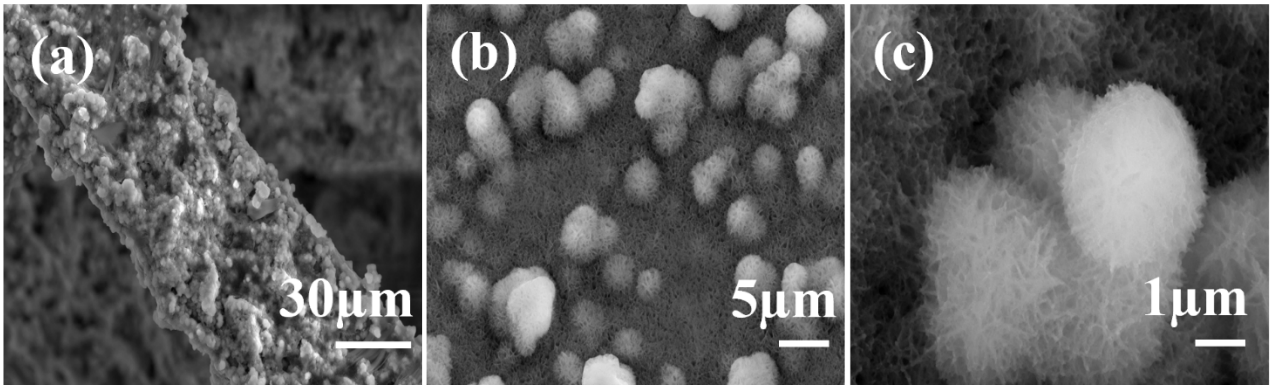

Fig. S3. (a-c) SEM images of NiS/Ni foam with increasing magnification.

7. Effect of concentration of Ru on HER activity of NiS/Ni foam

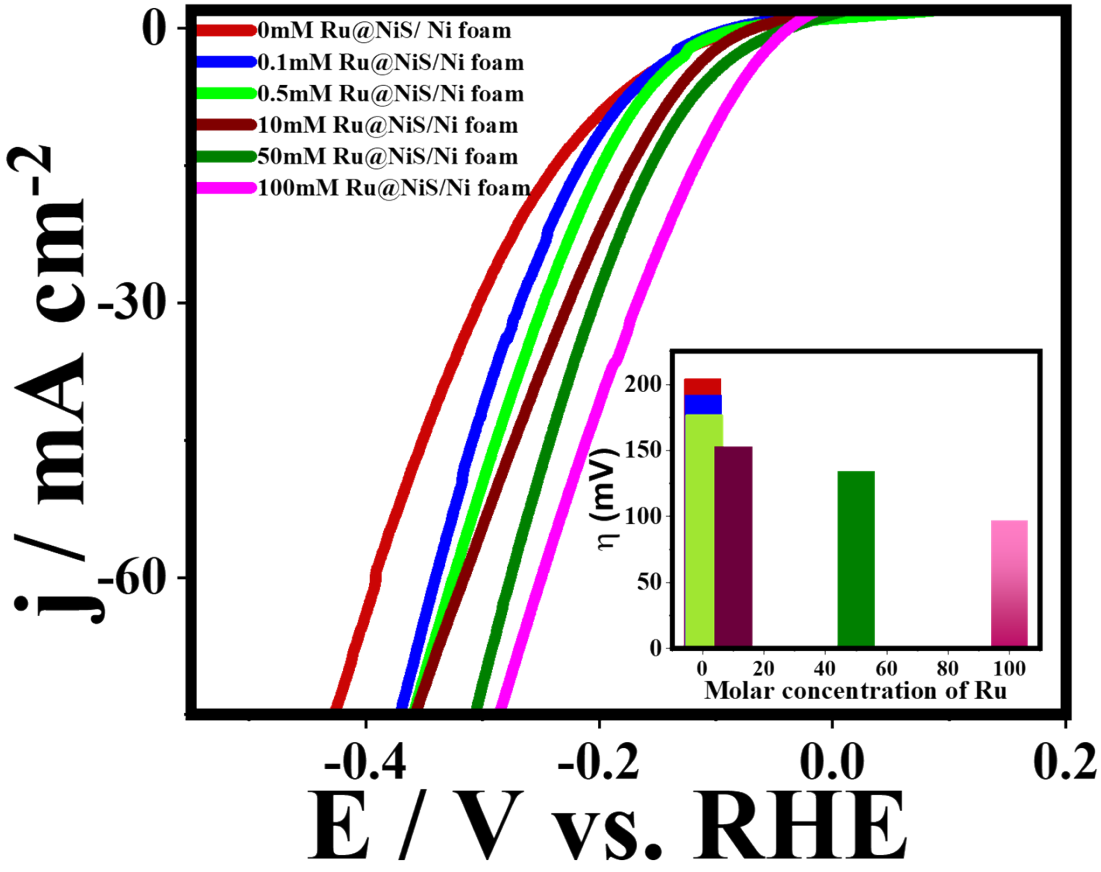

Fig.S4. LSVs of Ru@NiS (0mM, 0.1mM, 0.5mM, 10mM, 50mM & 100mM) in 1M KOH acquired with a scan rate of 5 mV s^{-1}

8. Calculation for Electrochemical Active Surface Area

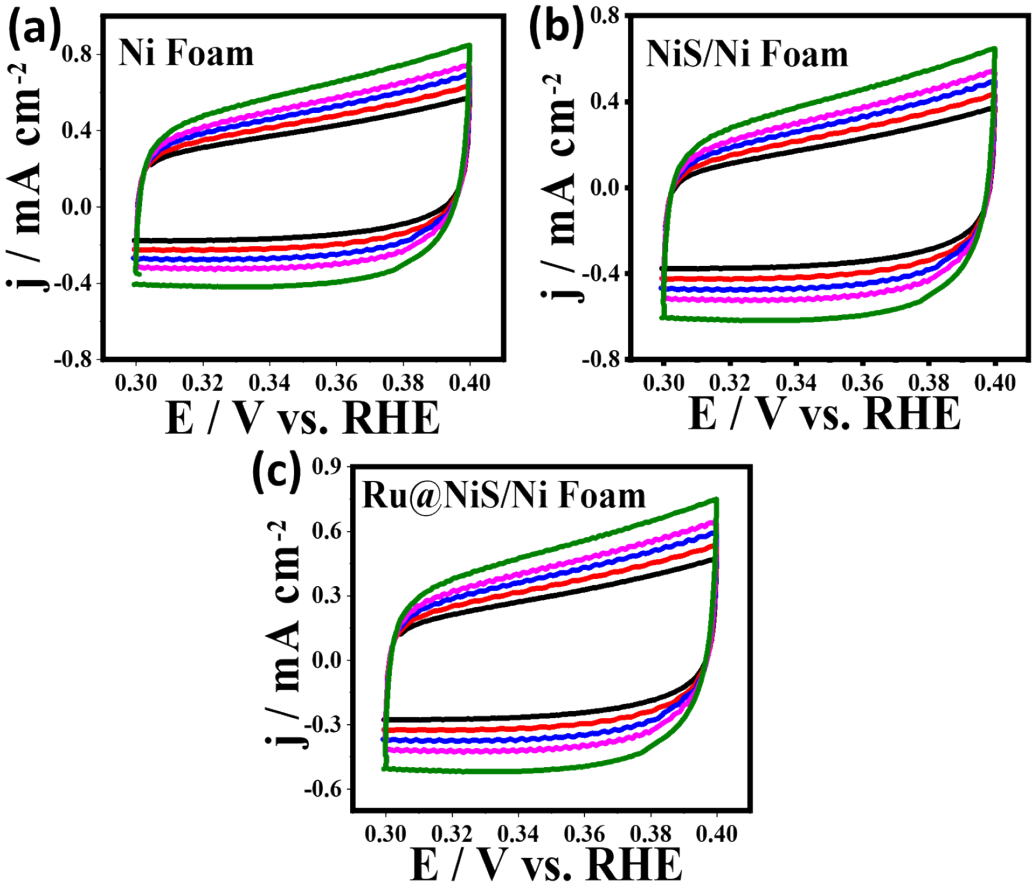

Fig. S5. (a-c) CVs of Ni foam, NiS/Ni foam and Ru@NiS/Ni foam with increasing scan rates from 20 mV/s to 100 mV/s in 1M KOH.

9. Comparison of admittance, phase angle and angular frequency

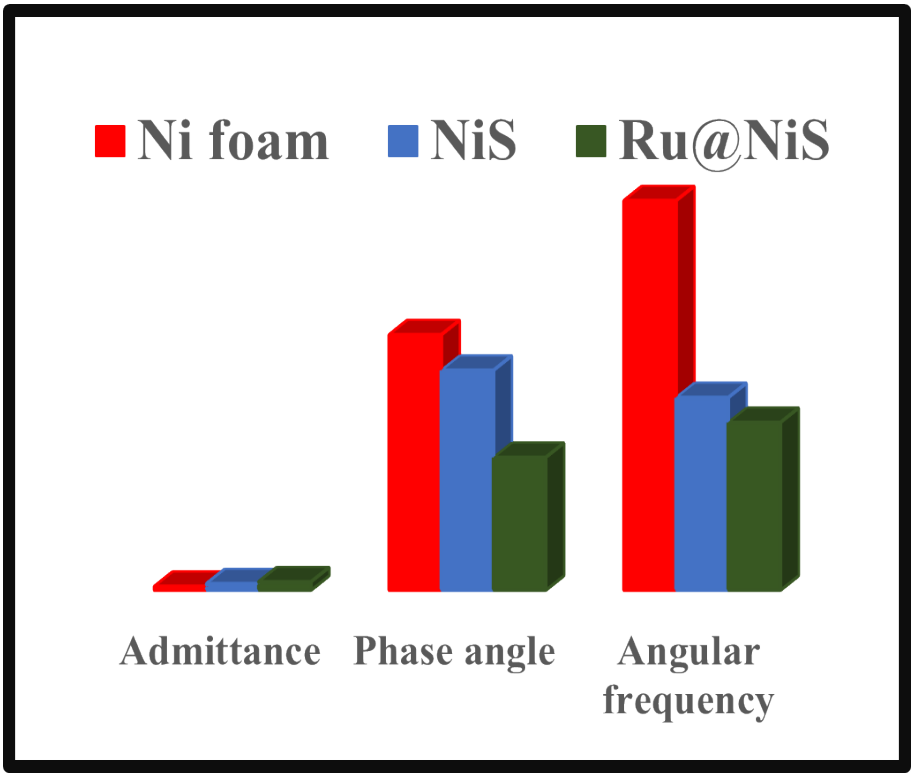

Fig. S6. Comparison representation of admittance, phase angle and angular frequency of Ni foam, NiS/Ni foam and Ru@NiS/Ni foam

10. **Reproducibility of Ru@NiS/Ni Foam electrodes for HER:**

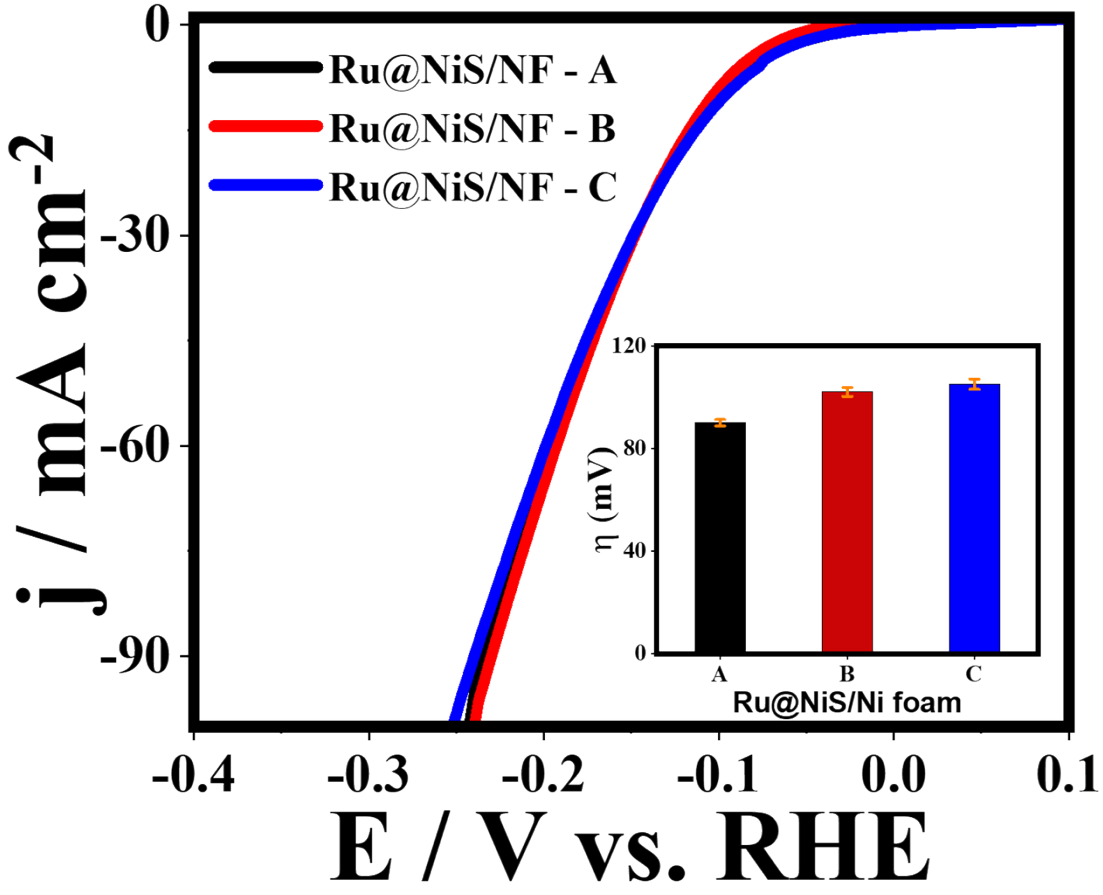

Fig. S7. LSVs of three brand new Ru@NiS/Ni Foam electrodes in 1M KOH.

(Inset: Reproducibility of overpotential of Ru@NiS/Ni Foam for HER)

11. Determination of Turn Over Frequency

At first, assuming each ruthenium atoms in the catalyst formed one active centre. The numbers of Ru atoms number in Ru@NiS/NF catalyst were calculated from the Ru molar mass and Ru concentration on Nickel foam, which derived from the XPS results. The Ru content of catalyst revealed by XPS measurement was 24.7%. Thus, the TOF the Ru@NiS/NF electrocatalyst was calculated according to the equation (3).

TOF (H_2 s^{-1}) = Total H_2 turnovers per geometric area / Active sites per geometric area (3)

The number of total H_2 turnovers per geometric area was calculated from the current density (J) for the HER-LSV polarization:

Total H_2 turnovers per geometric area = J X N_A / F X n

Where, j = current density, N_A= Avogadro number, F = Faraday constant, n = Number of electrons

$= 1.56 \text{ X } 10^{23}$ H_2 s^{-1} per mA/cm^2 (4)

Active sites per geometric area = 20 mM X 24.7% X $6.022 \text{ X } 10^{23}$

$= 29.7487 \text{ X } 10^{20}$ Ru site cm^{-2} (5)

Finally, the TOF of Ru@NiS/NF can be obtained via the current density from the HER- LSV polarization curves and according to (6):

$TOF_{0.068V} = 1.56 \text{ X } 10^{23} / 29.7487 \text{ X } 10^{20}$ (6)

$= 0.00052 \text{ X } 10^5$ s^{-1}

$=52$ s^{-1}

12. Stability test

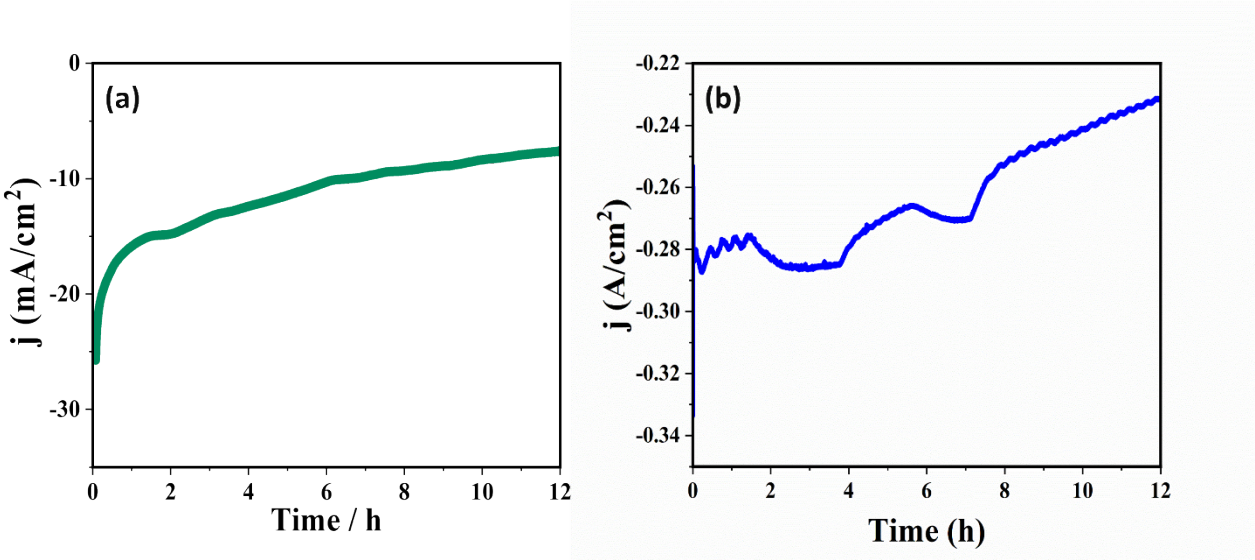

Fig. S8. CA response of Ru@NiS/Ni foam at (a) 1.2 V & (b) -2 V vs. Hg/HgO in 1 M KOH

13. Post reaction analysis

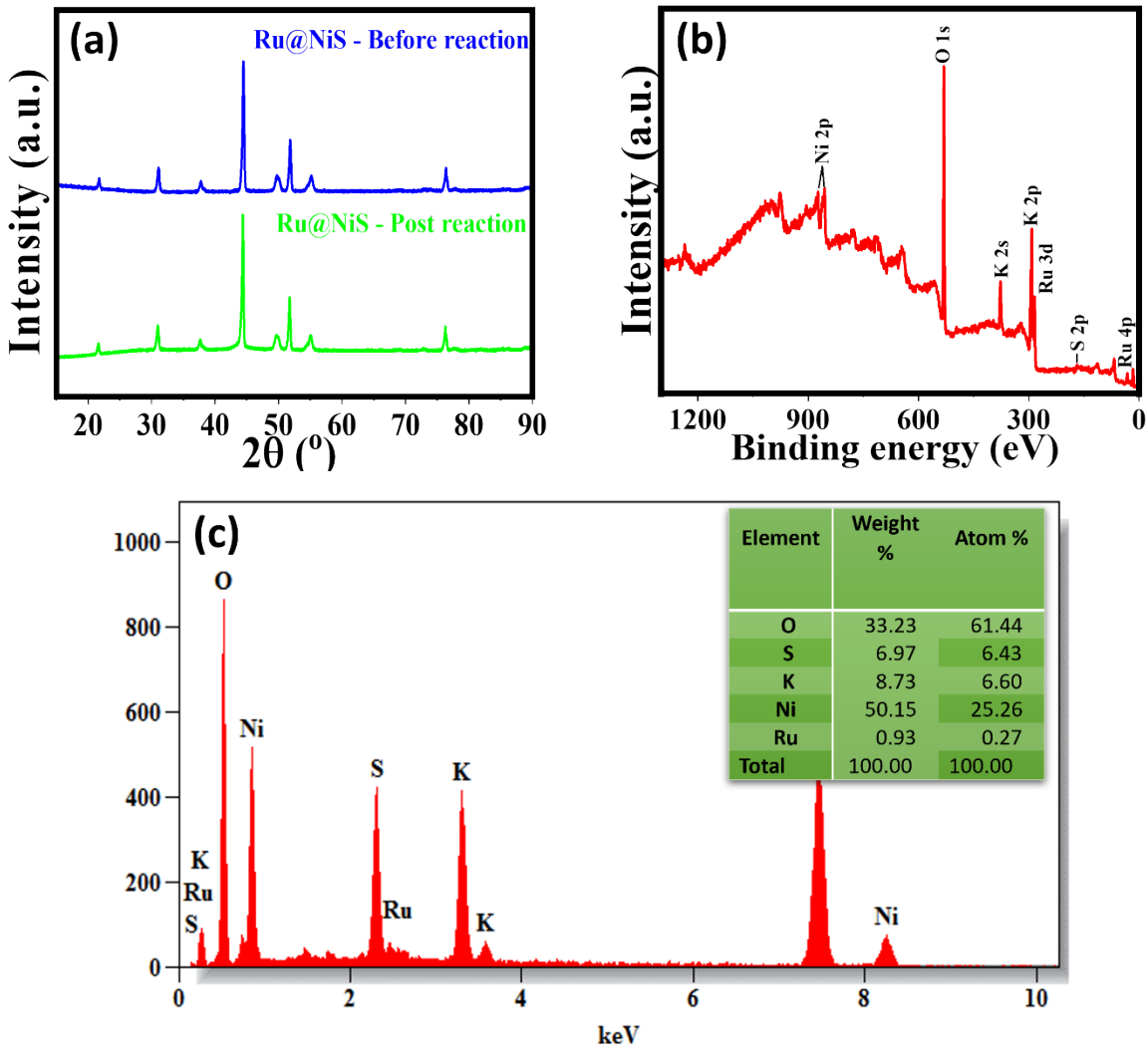

Fig. S9. (a) XRD of Ru@NiS/Ni foam before and after chronoamperometry, (b) XPS survey spectrum, (c) EDS spectrum and elemental composition of Ru@NiS/Ni foam after 12 hours of chronoamperometry test.

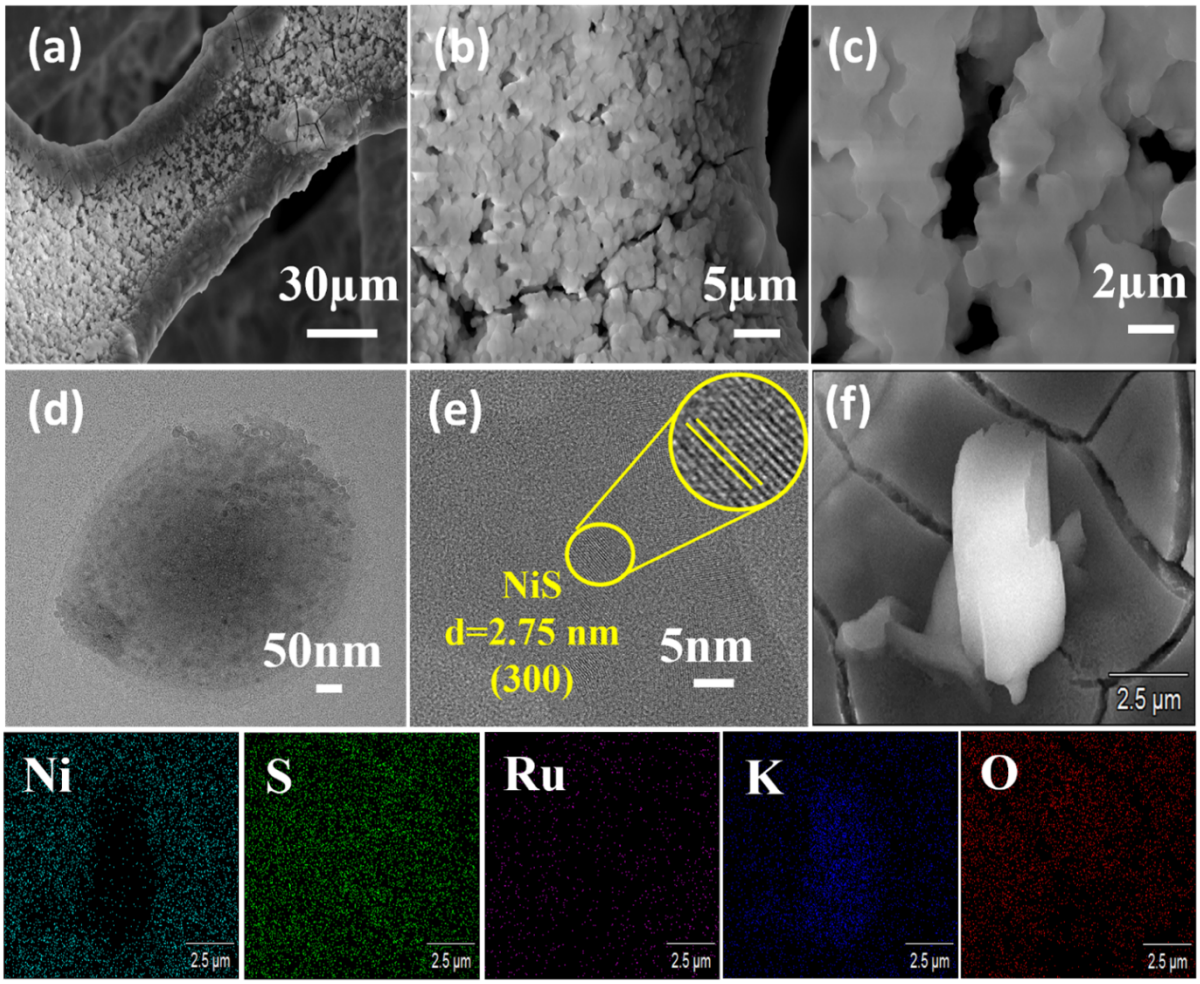

Figure S10. (a-c) SEM images. (d) TEM image and (e) HRTEM image. (f) SEM image of Ru@NiS/Ni foam where EDS were performed with corresponding mapping of elements after 12 hours of chronoamperometry towards HER.

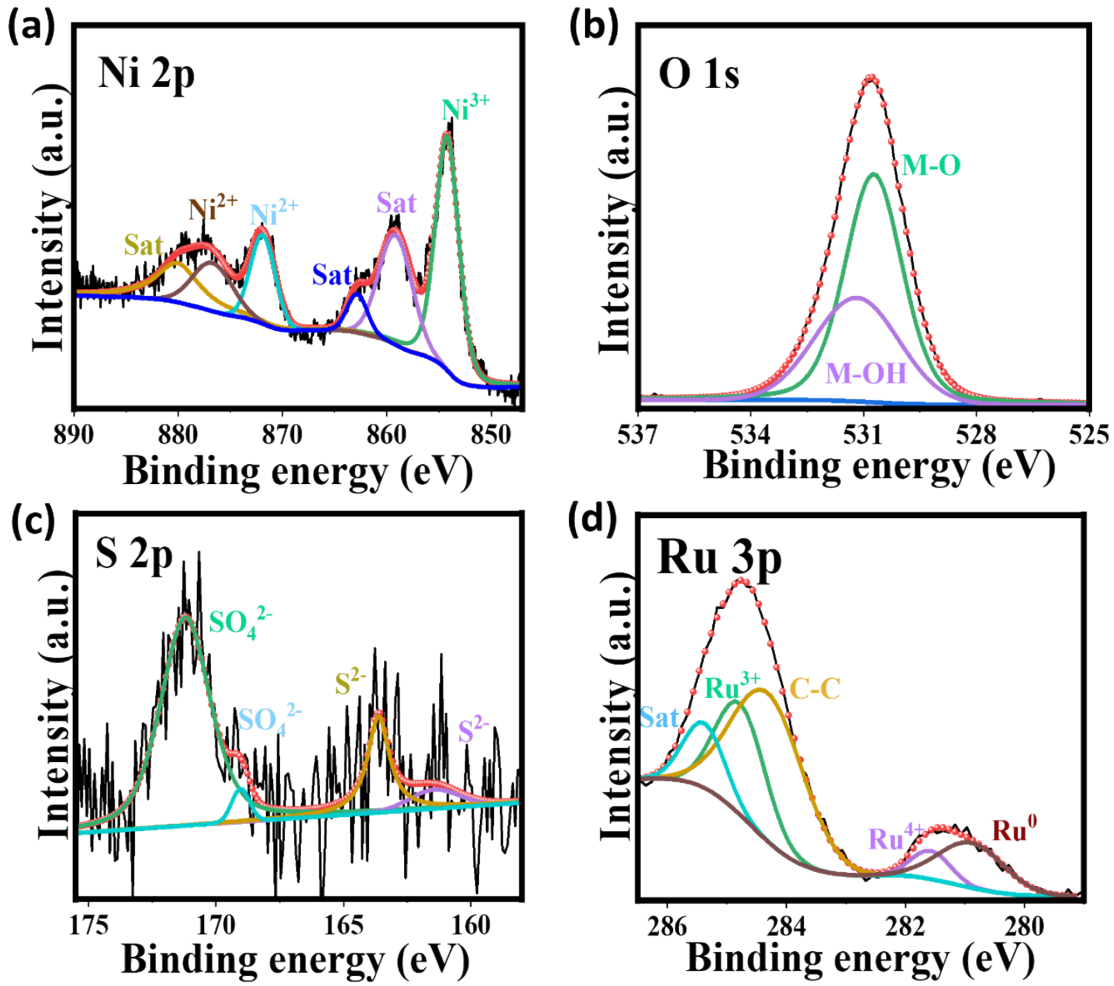

Figure S11. XPS spectra of (a) Ni 2p, (b) O1s, (c) S 2p & (d) Ru 3d in Ru@NiS/Ni foam after HER studies

14. Comparison of HER activity of Ru@NiS/Ni foam with other recently reported Ni based electrocatalysts at 10 mA/cm^2 in alkaline medium.

Catalysts	Overpotential (mV)	References
Ru@NiS/Ni foam	68.8	This work
$Fe_xNi_{3-x}S_2$@NF	72	[S1]
ReS_2/NiS/NF	78	[S2]
Zn-Ni_3S_2/NF	78	[S3]
$Ni_{0.67}Co_{0.33}/Ni_3S_2$@NF	87	[S4]
Vs-Ni_3S_2/NF	88	[S5]
MoS_2/Ni_3S_2	89	[S6]
Ni-S-OH/Ni foam	110 @ 100 mA cm^{-2}	[S7]
$NiS_2/CoS_2/MoS_2$	112	[S8]
MoCoNiS@NF	114	[S9]
Ni_3S_2/VG@NiCo LDHs	120	[S10]
P-$CoNi_2S_4$ YSSs	135	[S11]

$NiWO_4/Ni_3S_2$	136	[S12]
Mo-NiP_x/NiS_y	137	[S13]
NiS_2/MoS_2/CNTs	149	[S14]
Cu_2S-Ni_3S_2/NF	149	[S15]
Ni/NiS/P,N,S-rGO	155	[S16]
$CoNi_2S_4/g$-C_3N_4	160	[S17]
Co-Ni_3S_2	192	[S18]
Co-N-Ni_3S_2/Ni foam	215	[S19]

References

S1. B. Fei, Z. Chen, J. Liu, H. Xu, X. Yan, H. Qing, M. Chen and R. Wu, *Advanced Energy Materials*, 2020, 10, 2001963–2001963.

S2. Y. Liu, H. Zhang, Y. Zhang, W. Song, Z. Hou, G. Zhou, Z. Zhang and J. Liu, *Chemical Engineering Journal*, 2023, 451, 138905–138905.

S3. W. He, H. Liu, J. Cheng, J. Mao, C. Chen, Q. Hao, J. Zhao, C. Liu, Y. Li and L. Liang, *Nanoscale*, 2021, 13, 10127–10132.

S4. Z. Wu, Y. Feng, Z. Qin, X. Han, X. Zheng, Y. Deng and W. Hu, *Small*, 2022, 43, 2106904

S5. D. Jia, L. Han, Y. Li, W. He, C. Liu, J. Zhang, C. Chen, H. Liu and H. L. Xin, *Journal of materials chemistry. A, Materials for energy and sustainability*, 2020, 8, 18207–18214.

S6. J. Zhang, Y. Zheng, J. Wang, Y. Geng, B. Zhang, J. He, J. Xue, T. Frauenheim and M. Li, *Small*, 2021, 10, 2006730.

S7. S. Anantharaj, H. Sugime and S. Noda, *Chemical Engineering Journal*, 2021, 408, 127275.

S8. Y. Zhang, M. Shi, C. Wang, Y. Zhu, N. Li, X. Pu, A. Yu and J. Zhai, *Science Bulletin*, 2020, 65, 359–366.

S9. R. He, Pitchai Thangasamy, J. Wu, K. Yu, X. Yu, W. Tang, D. Quiroz, Deema Alyones, Z.

Chen, H. Luo and M. Zhou, *Electrochimica Acta*, 2023, 470, 143342–143342.

S10. X. Zhang, J. Fan, X. Lu, Z. Han, C. Cazorla, L. Hu, T. Wu and D. Chu, *Chemical Engineering Journal*, 2021, 415, 129048.

S11. X. Lu, Song Lin Zhang, Wei Lok Sim, S. Gao and W. David, *Angewandte Chemie International Edition*, 2021, 60, 22885–22891.

S12. S. Huang, Y. Meng, Y. Cao, F. Yao, Z. He, X. Wang, H. Pan and M. Wu, *Applied Catalysis B: Environmental*, 2020, 274, 119120–119120.

S13. J. Wang, M. Zhang, G. Yang, W. Song, W. Zhong, X. Wang, M. Wang and T. Sun, *Advanced Functional Materials*, DOI:https://doi.org/10.1002/adfm.202101532.

S14. G.-L. Li, Y.-Y. Miao, X.-Y. Qiao, T.-Y. Wang and F. Deng, *Applied Surface Science*, 2023, 615, 156309–156309.

S15. K. S. Bhat and H. S. Nagaraja, *ChemistrySelect*, 2020, 5, 2455–2464.

S16. M. Barakat, Mohamed Reda Berber, Y. Yamauchi, Amir Pakdel, R. Cao and U.-P. Apfel, *ACS Applied Materials & Interfaces*, 2021, 13, 34043–34052.

S17. R. Zahra, E. Pervaiz, M. M. Baig and O. Rabi, *Electrochimica Acta*, 2022, 418, 140346.

S18. Y. Li, Y. Duan, K. Zhang and W. Yu, *Chemical Engineering Journal*, 2022, 433, 134472.

S19. X. Du, G. Ma and X. Zhang, *Dalton Transactions*, 2021, 50, 8955–8962.